# A New Climatology for Investigating Storm Influences in and on the Extratropics

MIKE BAUER

*Department of Applied Physics and Mathematics, Columbia University, New York, New York*

GEORGE TSELIOUDIS

*NASA Goddard Institute for Space Studies, New York, New York*

WILLIAM B. ROSSOW

*Cooperative Remote Sensing Science and Technology Institute, City College of New York, New York, New York*

(Manuscript received 9 September 2015, in final form 18 March 2016)

ABSTRACT

The NASA Modeling, Analysis, and Prediction (MAP) Climatology of Mid-Latitude Storm Area (MCMS) project is a set of tools for examining midlatitude cyclones in model-generated data. The MCMS software has two primary tasks. The first task identifies and tracks likely cyclones in sea level pressure fields. Special care is taken to minimize the known problems of this approach near steep or high topography. The second task finds the outermost closed pressure contour that uniquely surrounds each cyclone center, or collection of centers in the case of multicenter cyclones. This enclosed area is then used as a rough proxy for the domain over which a cyclone influences its immediate environment. Here the MCMS software is applied to several decades of reanalysis data. These results are shown to be consistent with the findings of a recent intercomparison of cyclone-finding methods. Besides providing details concerning cyclone storm area, the MCMS software departs from other cyclone-finding methods by providing a comprehensive record concerning every cyclone it processes. The MCMS software also provides extensive diagnostics about the actions of specific operations (filters) and adjustable parameters. The benefits of this accounting are demonstrated and discussed, as are those related to the use of cyclone storm area as a tool for climate research. MCMS datasets are available for several reanalysis products, as is the MCMS software itself, including the source code needed to generate new MCMS datasets and utilities for working with existing ones.

## 1. Introduction

In this paper, we describe a new system for mapping the area of influence surrounding baroclinic extratropical cyclones (or just cyclones) using gridded sea level pressure data.

Meeting this goal depends on having a procedure for finding, tracking, and delineating cyclones. The basic tools for this have been developed numerous times using a variety of approaches (e.g., Murray and Simmonds 1991; Sinclair 1994; Hoskins and Hodges 2002; Wernli and Schwierz 2006; Inatsu 2009; Hewson 2009; Hanley and Caballero 2011). A recent intercomparison project concerning such efforts, the Intercomparison of Mid-Latitude Storm Diagnostics (IMILAST; Neu et al. 2013, hereinafter Neu13), concluded that the cyclones identified by these methods are statistically similar (patterns of occurrence, attribute means, etc.). However, upon closer inspection, and especially at the level of individual cyclone tracks, this accord was far less evident (Neu13).

Reconciling these differences requires more information than can be gleaned from the retained cyclone tracks alone. Unfortunately, these sorts of detailed diagnostic data are rarely available. Lacking this, Neu13 could only point to the interplay between the fixed properties of the analysis and the changing state of the dataset as a possible cause of this uncertainty.

Indeed, much of this uncertainty surely lies in the specific criteria each method uses to distinguish cyclones from the other patterns of spatiotemporal variability inhabiting the climate system and its related datasets. The central challenge here is that cyclones exhibit a diversity

*Corresponding author address*: Mike Bauer, NASA Goddard Institute for Space Studies, 2880 Broadway, New York, NY 10025. E-mail: mpb20@columbia.edu

DOI: 10.1175/JAMC-D-15-0245.1

© 2016 American Meteorological Society

Unauthenticated | Downloaded 03/15/22 04:05 PM UTC

of form and behavior that defies simple, universal, and unambiguous characterization.

This means that any search criteria that we might devise is bound to be approximate and therefore to offer only a partial sample of the true cyclone population, favoring some cyclones more than others (bias) and admitting noncyclone features (contamination). Moreover, the inconstant and uneven nature of the underlying distribution is apt to alter the representativeness of our sample in complicated ways. In short, it seems reasonable to conclude that all cyclone climatologies contain some conditional uncertainty and bias.

While we cannot reasonably rid ourselves of these methodological artifacts, we can try to document their existence and influence. To address this challenge we have created a new tool for cyclone finding, tracking, and delineation. These tools form the basis for the NASA Modeling, Analysis, and Prediction (MAP; http://map.nasa.gov/overview.html) Climatology of Mid-Latitude Storm Area (MCMS) project.

As noted earlier, the basic tools for creating cyclone datasets already exist. MCMS distinguishes itself from these previous efforts because it retains the causal sequence of factors (both algorithmic and environmental) affecting the acceptance or rejection of every candidate cyclone center processed by the software. This algorithmic trace is part of a rich catalog of cyclone-related metadata stored by MCMS (e.g., storm geometry, travel, and proximity to, and potential connections with, other systems). This added scope, besides its obvious diagnostic and elucidative utility, makes MCMS data more useful than a simple list of cyclone positions.

For example, consider the correspondence between nearby cyclone activity and some other local event of interest (e.g., extremes or weather states; Tselioudis et al. 2000; Hawcroft et al. 2012; Romanski et al. 2012). For this purpose, MCMS storm location and extent serve as an alternative, and possibly more informative, marker for local cyclone activity than does the presence of a nearby cyclone center [i.e., areas rather than points, as in Pfahl and Wernli (2012)]. MCMS data, in contrast, allow for additional safeguards and avenues of investigation. For example, they easily identify cases where the initial analysis suggested that no cyclone was present, when in fact one was detected and discarded by the MCMS algorithm.

Last, we note that the MCMS tools work closely together and are easy to use (i.e., documented, examples). In addition to creating cyclone datasets, MCMS offers a selection of utilities for manipulating and exploring the dataset to suit various research needs (e.g., partitioning, reorganizing and statistics, maps, histograms, composites). Information based on these tools is displayed throughout this paper. The MCMS software is also modular, and thus easy to modify and extend. Last, the MCMS software and its related datasets are freely available.

We take up the MCMS methodology in the first sections of the paper, along with a general comparison with IMILAST via Neu13. In later sections, we discuss some results from applying the MCMS software to several decades of reanalysis data. Last, we discuss possible uses for MCMS data and provide details on how to obtain MCMS data and software.

## 2. Methods

### a. Data

The MCMS software is intended for use on a variety of gridded SLP data sources (e.g., climate and reanalysis models). The results presented in this study are based on the SLP values provided by the European Centre for Medium-Range Weather Forecasts (ECMWF) interim reanalysis (ERA-Interim, hereinafter ERAi; Dee et al. 2011). ERAi output offers a long record (1979–present) with sampling characteristics that are well suited to cyclone tracking: 6-hourly samples on a 1.5° latitude–longitude data grid. This is also the dataset used by Neu13.

### b. Cyclone finding, tracking, and delineation

The MCMS method, like many other methods of cyclone finding, is essentially a geophysically informed search algorithm. Ideally, the search criteria powering this algorithm are effective and easily implemented on readily available datasets (e.g., SLP). These criteria, and the manner of their application, vary from method to method as is discussed by Neu13. Here we discuss the specifics of the MCMS algorithm.

Before doing this, we will first address some general features of the MCMS tool set. Foremost among these is the idea that the software should rigorously document its actions. These log files have many uses. For example, the log files contain the algorithmic trajectory of every data point processed by the MCMS software. These log files can therefore be used to diagnose specific cases, such as why a particular cyclone was or was not identified and retained. Finally, the log files can be mined for summary statistics, histograms, and maps that document the algorithm's general behavior. The log files can also be used to quantify the effects of altering the algorithm, especially the selection criteria, or applying it to a new SLP dataset. Information derived from these log files is used throughout the following text. Another general feature of the MCMS software is that it derives many of

Unauthenticated | Downloaded 03/15/22 04:05 PM UTC

its key parameters directly from the SLP dataset being analyzed.

#### 1) CENTER FINDING

This section describes the first stage of the MCMS cyclone-finding algorithm. The key concept here is that cyclones usually manifest themselves as distinct synoptic spatial-scale areas of lower pressure (i.e., depressions). As a practical matter, the MCMS method uses local minima in the SLP field as a proxy for these depressions. These minima are found by scanning the data grid sequentially over time and compiling a list of candidate cyclone centers. In synoptic terms, this evaluation spans a relatively short distance (here a radius of 300 km, the inner radius). Bilinear interpolation is used to adjust the data-grid SLPs to this radius.

After the initial scan, the candidate centers are sorted by SLP (from low to high) and injected into the filter pipeline described below. Filtering is necessary because the initial scan gathers many noncyclone SLP minima (e.g., heat lows). These filters generally target noncyclone characteristics, although the lack of key cyclone characteristics triggers others. Figure 1a provides an example of the typical mixture of retained (black and green boxes) and discarded (orange circles) centers. Note that the status of a center as being retained or discarded is somewhat provisional because the next stage of MCMS cyclone finding (tracking) can override these judgments. In any case, all candidate centers are stored along with a meaningful flag value.

The broadest set of center-finding filters removes overly shallow or overly localized SLP depressions. The most universal of these filters discards candidates enclosed by pressures greater than 1020 hPa (using the inner-radius SLPs). For the most part, these centers represent shallow (<1 hPa) small-scale dimples along the periphery of large high pressure systems.

The remaining candidates are then compared to a set of SLP thresholds that depend on hemisphere, season, and topography. These thresholds vary from 960 to 1010 hPa and are lower during warm seasons and over higher topography (i.e., exceeded more easily).

Candidates thus flagged are examined more closely. For example, their minimum status is rechecked at a wider distance (here a radius of 600 km, the outer radius). Candidates judged as nonminima at this scale are discarded, as are those with little east-to-west or north-to-south contrast between their outer and central SLPs (<~4-hPa average difference). Many of these discards occur over land, especially near high topography, where their sporadic occurrence is consistent with small-scale noise. Candidates that would otherwise be discarded are retained if 1) their central SLP is less than those of all enclosed data grids (i.e., not just at the outer radius, depressionlike) or 2) most of the enclosed data grids that are lower pressure fall on the poleward side of the center (>75%, open-wave-like). These exceptions are restricted to oceanic centers because of the increased spatial variability of SLP over land.

Another filter class targets overly recurrent centers, such as those associated with quasi-diurnal thermal lows. This filter depends on two ideas. The first idea is that multiple distinct cyclones are unlikely to visit the same location over a relatively short period. The second idea is that slow-moving cyclones are unlikely to remain stationary for more than a relatively short period. Neither statement is strictly true, which could make this filter overly aggressive. However, the MCMS track-finding algorithm can compensate for this by recovering discarded centers that can be placed into otherwise trackable cyclones. This filter only applies over land and is restricted to candidates with relatively elevated central SLPs for their setting (same thresholds as before). The key idea is to check the data grid of each current candidate for centers at the same local time but 2 days previously (i.e., −42, −48, and −54 h). This 2-day gap allows slow-moving cyclones time to move away and evade this filter. When recurrence is detected, the central SLPs of the conflicting current and past candidates are compared. When their absolute SLP difference is small (<5 hPa) the conflicting candidates are discarded under the premise that they lack the temporal development characteristic of cyclone behavior. These discards are concentrated around elevated topography during the daylight hours of the warm season.

The next filter targets data grids with inordinate center counts. This requires a special preliminary run of the center-finding algorithm with this particular filter disabled. These results are then examined for two types of outliers. The most problematic outliers are data grids with excessive center counts (above the 99th percentile). The other outliers represent data grids whose center count greatly exceeds those of its eight immediate neighbors. Together these outliers, which represent <1% of all center containing data grids, account for >11% of the total center count in the preliminary run.

The next filter type targets high-latitude candidates (>|60|°). One of these filters uses a special lookup table to flag candidates over high or steep topography. These candidates are discarded if any enclosed outer SLP is less than the central SLP (unless that data grid is already a retained center). A related filter targets candidates near and over Antarctica. Candidates over Antarctica are discarded if any enclosed outer SLP is less than the central SLP. Candidates from Antarctic coastal waters, in contrast, are discarded only if their

Unauthenticated | Downloaded 03/15/22 04:05 PM UTC

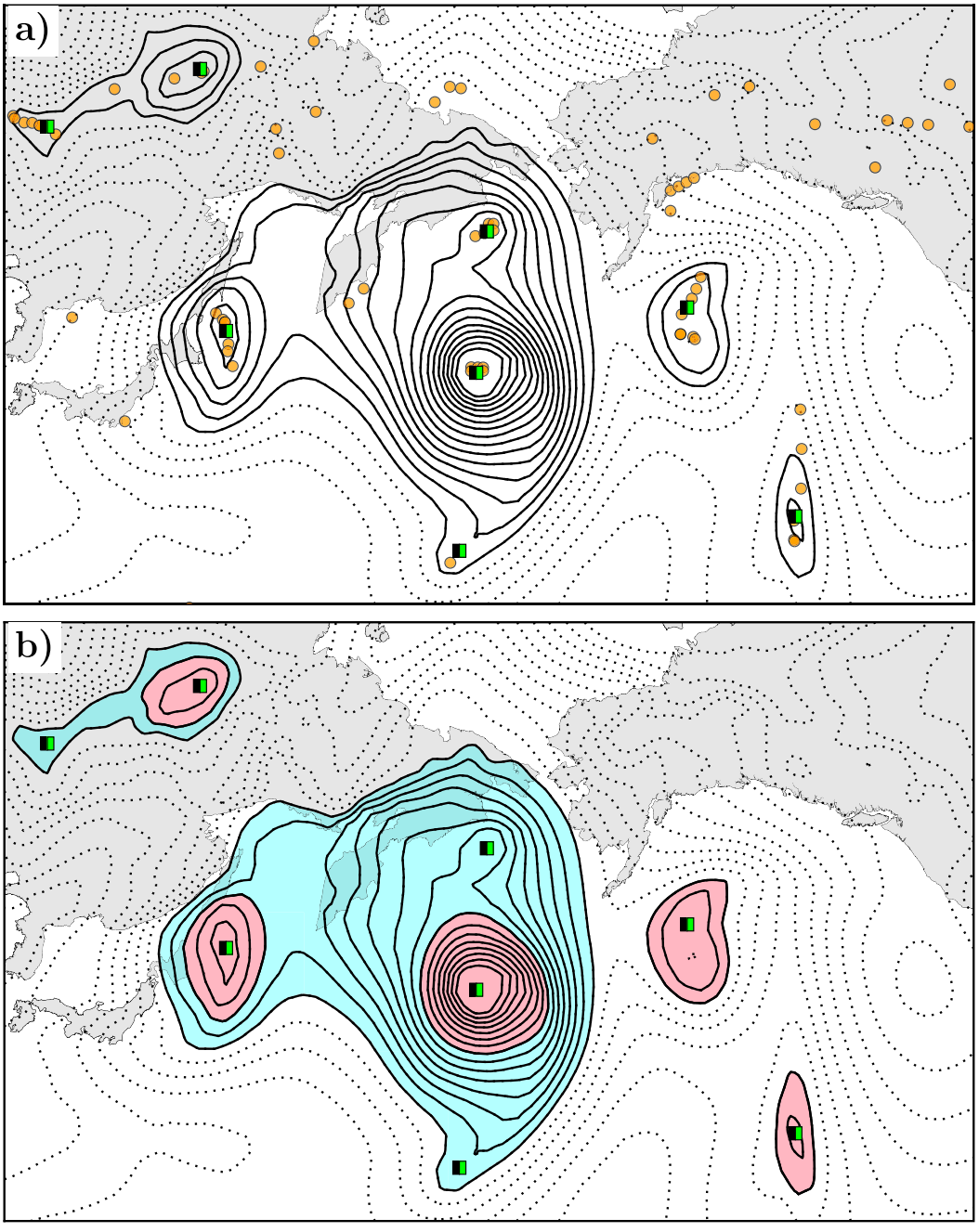


FIG. 1. A limited example of MCMS storm-area delineation. (a) The closed SLP contours (solid) enclosing one or more cyclone centers (black and green boxes). The associated discarded centers (orange circles) are also shown. (b) The flood-filled storm areas defined by the outermost closed contours containing one (red fill) or more (cyan fill) centers.

central SLP exceeds the time-average zonal-mean SLP for the current month, year, and latitude. These filters target spurious SLP minima that sometimes appear when legitimate oceanic cyclones interact with the steep coastal topography around Greenland and Antarctica (i.e., noise).

A final check ensures that the synoptic domain of each retained center is free of overlap with other candidate centers. Outside polar latitudes, this domain is roughly circular and set by a latitude-dependent zonal wavenumber (wavenumber 26 or ~300–700 km). Near the poles, a fixed value of ~300 km is used instead. Filtering

Unauthenticated | Downloaded 03/15/22 04:05 PM UTC

rules are then recursively applied to the candidate pool until all overlap is removed. During this process alternative solutions are considered to ensure retention of the lowest SLP candidates and a large final candidate pool. These discards occur mostly at high latitudes, over regions of complicated orography, and along the main storm tracks in proximity to another retained center. In the latter case, these discards often represent bends in the outer SLP contours of a cyclone (perhaps along frontal boundaries) and indistinct open waves.

The final candidate pool represents a small subset of the original data grids (about 47 centers per time step). Overall, the center-finding filters are least aggressive during the cold season over the midlatitude oceans and most active during the warm season over high topography and in the subtropics.

The final center-finding calculation simply fine-tunes the center position using a quadratic fit of the local SLP field. This yields a latitude–longitude pair located somewhere within the original center-containing data grid. This location, plus the date and time, are then used to make a unique center identifier (UCI). Everything is then stored in a file before advancing to the next time step.

#### 2) TRACK FINDING

The key concept behind this aspect of cyclone finding is that cyclones usually manifest themselves as traveling eddies that persist over a synoptic time scale (i.e., a cyclone track). In essence, track finding uses nearest neighbor and other similarity arguments to identify likely center-to-center connections over time. Key to this is a dissimilarity score that is calculated for each potential connection linking a current center to centers from the previous time step. Dissimilarity is based on three ideas: 1) close is best, 2) stay the course, and 3) change is gradual.

The close is best (CisB) criterion favors connections between nearby centers. As in other cyclone-tracking methods, the MCMS algorithm uses a maximum cyclone propagation speed (120 km $h^{-1}$ or 720 km over 6 h) to limit the pool of nearby candidate centers (e.g., Hodges 1999; Wang et al. 2006; Trigo 2006). The relative separation of each candidate connection, which is squared to place progressively greater weight on longer separations, is then used to find CisB [i.e., $(\text{separation}/\max\text{separation})^2$]. Connections with a CisB $> 1$ are ignored. The remaining CisB values have a unimodal distribution that is skewed toward zero (mode = 0.031 or ~125 km, median = 0.084 or ~210 km, and mean = 0.241 or ~350 km), with most potential connections falling well inside the maximum separation (<10% have a CisB > 0.45 or ~500 km). Elevated CisB values tend to occur where cyclones travel quickly (e.g., storm tracks) and near high or steep topography.

The next criterion is stay the course (StheC). StheC favors connections that extend tracks eastward. This depends on the direction of track propagation (bearing) for each connection. When the bearing is eastward (<180°), StheC is the absolute bearing differential with a purely eastbound track or $\text{StheC} = |(\text{bearing} - 90°)/90°|$ (i.e., StheC ranges from 0 to 1). Westward bearings are actively discouraged with a penalty that peaks for a purely westbound track or $\text{StheC} = 2 - |(\text{bearing} - 270°)/90°|$ (i.e., StheC ranges from 1 to 2). The distribution of StheC resembles that of CisB (mode = 0.032, median = 0.049, and mean = 0.235). Candidate connections have a strong eastbound tendency with 58% of all bearings falling between 45° and 135°. Note that westward connections (StheC > 1) are allowed and are most common at low and high latitudes and near high or steep topography.

The final dissimilarity criterion, change is gradual (CisG), favors connections between centers with nearly equal SLPs (i.e., small SLP tendencies). These tendencies are latitudinally adjusted in a manner akin to that used by Sanders and Gyakum (1980) to identify explosively developing or bomb cyclones. For our purpose, a large tendency is defined by the reference value $\Delta\text{SLP}_r = (2\,\text{hPa}\,\text{h}^{-1}\sin|\phi|)/\sin 60°$, where $|\phi|$ is the mean absolute latitude of the center. CisG simply compares the absolute SLP tendency of each connection with this reference or $\text{CisG} = |\Delta\text{SLP}|/(\Delta\text{SLP}_r \times \text{time step})$. Note that a CisG value of 1 represents a very large SLP difference of about 2 bergerons using the Sanders and Gyakum (1980) scale. However, this change happens during a single time step rather than over the original bomb criteria of 24 h. Thus, CisG > 1 are understandably rare (<3% of connections) and unwanted events (i.e., tropical cyclones). The very highest CisG values (>2) are generally found among connections between centers over high or steep topography and are therefore discarded. The distribution of the remaining CisG values is unimodal and strongly skewed toward zero (mode = 0.047, median = 0.137, and mean = 0.223). Hence, the SLP change implied by most candidate connections is far smaller than our modified bomb criteria. Indeed, roughly 90% of all CisG values (i.e., including values for rejected connections) are less than 0.5.

Once calculated, these criteria are then combined into a dissimilarity score for each potential connection or $\text{Ds}[\text{center}(t), \text{center}(t-1)] = (\text{CisB}^2 + \text{StheC}^2 + \text{CisG}^2)^{0.5}$. That is, Ds is a distance metric from an origin of sameness. Dissimilarity is most sensitive to the CisB criterion because of its interdependence with StheC, although it can be overcome by a combination of StheC and CisG.

Unauthenticated | Downloaded 03/15/22 04:05 PM UTC

Thus for example, a connection with a large course change and a small separation is favored over another connection with a smaller course change and a large implied displacement. The distribution of Ds is unimodal and strongly skewed toward zero (mode = 0.08, median = 0.3, and mean = 0.5). That is, most potential connections involve relatively similar centers.

Track selection works by considering all possible connections (limited by travel distance via CisB and extreme SLP tendency by CisG) and selecting the tracks that minimize the overall track Ds. This proceeds in a time-forward fashion and always considers connections with preexisting tracks first, and then works from the lowest to highest SLP among the other centers. In practice dissimilarity is rarely needed; ~82% of cases involve one or no connections (97% have two or less). However, when multiple connections are possible, the mean Ds of the chosen connection (~0.3) is less than half that of the rejected connections (~0.7). In other words, dissimilarity-based tracking decisions are generally clear-cut. This is especially true in the oceanic storm tracks where multiple connections are often symptoms of secondary cyclogenesis and track mergers. The situation differs over high or steep topography because of the prevalence of centers that are relatively isolated from other centers in both time and space (i.e., unlikely cyclone centers). For example, most untrackable centers, those with no potential connections in the previous or following time step, are found in these areas. Centers with multiple connection possibilities are far less common there as well. Indeed, high topography connections generally have high Ds values because of high implied travel speeds or large changes in direction or SLP (tendency). These findings underscore the general difficulty with SLP-based cyclone tracking over high or steep topography.

Two additional track-finding operations remain. The first occurs whenever a new track is established between two centers. When this happens, an attempt is made to extend the track back in time using the pool of centers discarded during center finding. In this case, the CisB radius of the first center in the track is used to look for candidates among the discards from the previous time step. Discarded candidates with concurrent retained centers within the CisB radius are ignored to avoid track collisions (i.e., overly close centers). The tracking rules discussed above are then applied, and if a connection is made, the discarded candidate becomes the new first center of the track. A similar check occurs whenever a track cannot be extended into the future. In this case, the discarded centers from the next time step are used, and if a connection is made, the track is extended into the future. In essence, these recovery procedures overrule the center-finding decision to discard a center in light of its potential to extend an existing cyclone track. These track adjustments are most common over high topography and help carry cyclone tracks over topographic obstacles.

A final set of whole-track filters is then applied. For the most part, these filters are quasi-redundant such that suppressing one simply evokes another more often and results in only modest changes in the results. The most basic of these filters drops all untrackable centers (about 9% of the initial center-finding centers). This filter is most active over high elevations and in tropical regions where no possible connections exist within the limits set by the MCMS software. Other discarded tracks include those that 1) are purely tropical ($<|30|°$, this removes another 8% of the initial centers); 2) are too short in duration (<24 h, ~16% of the initial centers); 3) have too-high pressure (track minimum SLP > 1010 hPa, ~4% of the initial centers); 4) have low mobility (failing to move a minimum displacement from their starting point, <200 km, 7% of the initial centers). Together these tests reduce the total track count by 40%.

Last, a unique storm identifier (USI) is assigned to each kept center. This is simply the UCI of the first center in the track. Tracking retains about 85% of the initial center-finding centers or about 41 centers per time step. As with center finding, these filters are most aggressive away from the midlatitude oceans. As before, the retained and discarded centers are stored to a file.

Because of the way tracks are assembled it sometimes happens that two tracks compete for a common center (center A), with one track (track A) getting that center and the other (track B) not. In the event that track A is removed by filtering, the potential connection between center A and track B will go unrealized. To alleviate this, the tracking algorithm is rerun using the initial tracks and tracking discards. In this case, the tracking discards are only allowed to extend or improve tracks (no new tracks). This allows track B to recapture center A and all the connections that may follow. These track adjustments mostly occur over the oceanic storm tracks and near the semipermanent lows.

### 3) CYCLONE DELINEATION

In this section, we move beyond representing cyclones as points (i.e., cyclone centers) in favor of a treatment that accounts for their individual size and shape. For this, the MCMS software uses the largest set of closed isobars enclosing each cyclone center. This idea is not new. For example, tropical cyclones are sometimes measured by their radius of outermost closed isobar (ROCI; Merrill 1984) or their pressure of outermost closed isobar (POCI; Kimball and Mulekar 2004).

Unauthenticated | Downloaded 03/15/22 04:05 PM UTC

Wernli and Schwierz (2006) and Hanley and Caballero (2011) apply similar ideas to extratropical cyclones. However, these studies use closed SLP contours as a way to locate cyclones and to improve tracking, whereas for the MCMS software, closed SLP contours define the cyclone storm area (SArea, loosely the area of cyclone influence).

SArea is computed on a polar azimuthal equal-area projection rather than on the data grid as with center and track finding. To do this, the SLP field is interpolated onto a separate hemispheric working grid (here 250 × 250). Each hemisphere is then contoured separately using a variable contour interval. The contouring always starts at the hemispheric minimum SLP. An interval of 1 hPa is then used to extend the contouring up to 980 hPa. A finer interval of 0.5 hPa is used after that to capture closed contours at higher SLPs. The resulting contours are stored individually as a vector of vertices.

Contours unlikely to be cyclone related are then removed; for example, contours lacking an enclosed cyclone center. Contours enclosing high pressure systems and those with excessively long perimeters (>14 000 km) are also discarded. Contours with more than 75% of their enclosed surface area inside |30|° latitude, or any area inside |15|° latitude, are also discarded (i.e., tropical features).

The remaining contours contain one or more cyclone centers. Hanley and Caballero (2011) refer to these as single-center (SCC) and multicenter (MCC) cyclones. We will use these terms as well. It sometimes happens that a cyclone center has no enclosing contours (e.g., an open-wave system). Although the MCMS software cannot define the storm area for these centers, they are retained in the dataset under a special ''empty'' category. Figure 1a illustrates this aspect of contour filtering.

The software then looks for the outermost (highest pressure) contour that is unique to each center (from lowest to highest SLP). If one is found, a raster area fill is applied and stored (using the data grid). This is the attributed SArea for that center. SArea can be further differentiated by whether the center is an SCC or part of an MCC. For SCC centers, SArea (or SArea_SCC) is also the total storm area. For MCC systems, the total storm area (SArea_MCC) is a combination of areas that are unique to specific centers (SArea_Embedded) and the remaining space between and around these centers (SArea_Shared). The example shown in Fig. 1b depicts both SArea_SCC and SArea_Embedded with red shading and SArea_Shared with cyan shading. Sometimes it is convenient to treat MCC systems as a whole (i.e., as an SCC). This is done by selecting the lowest SLP center as the ''primary'' for the system. In this case, the primary center retains some of its properties (e.g., location, track, and central SLP) and acquires other properties from the MCC system (e.g., SArea_MCC becomes SArea_SCC).

### c. Comparison with IMILAST

We can now place MCMS into the context of other cyclone-finding schemes. For this we appeal to IMILAST (Neu 13). The IMILAST experimental design calls for some comparisons to exclude centers found over high topography or at low latitudes (>1000 m and <|30|° latitude). Unless otherwise stated, the following comparisons use this restricted set of MCMS data.

#### 1) CASE STUDIES

To start, we will use the detailed log files kept by MCMS to examine two case-study cyclones provided by IMILAST.

The MCMS track for the first of these storms, the Klaus cyclone of 22–27 January 2009, can be seen in Fig. 2a. Klaus spent its initial phase as a fast-moving open-wave cyclone (Liberato et al. 2011). MCMS recorded this activity as a discontinuous, and therefore untrackable, trail of discarded centers from early 22 January into 23 January. Around this time Klaus entered a period of rapid development and became a more defined SLP minimum (Liberato et al. 2011). This allowed MCMS and many IMILAST methods to form a track for Klaus on midday 23 January and extend it forward into southern France (track A in Fig. 2a). At this point, Klaus (track A) encountered another SLP minimum located just upstream over the Gulf of Genoa. The complexity of this situation led to a great deal of intermethod divergence among the IMILAST methods (Neu13). In the case of MCMS, all three centers related to the Genoa minimum were discarded because of their shallow nature and proximity to steep coastal topography (three Xs in Fig. 2a).

The next time step was more problematic for MCMS because a rival concurrent track made a sharp westward excursion into the path of track A (see track B, the open circle nearest the Gulf of Genoa in Fig. 2a). Two key attributes of this excursion are important here: 1) it was the lowest SLP center in the region, and 2) it was part of track B rather than track A (via dissimilarity). MCMS tracking decisions are ordered by the SLP of the time-forward connecting center. Thus the excursion of track B, and the subsequent discarding of all centers within the surrounding synoptic region, effectively starved track A of all forward connections.

This single decision results in a three-track Klaus solution for MCMS (tracks A, B, and C in Fig. 2a). To demonstrate this, we redid the Klaus tracking but

Unauthenticated | Downloaded 03/15/22 04:05 PM UTC

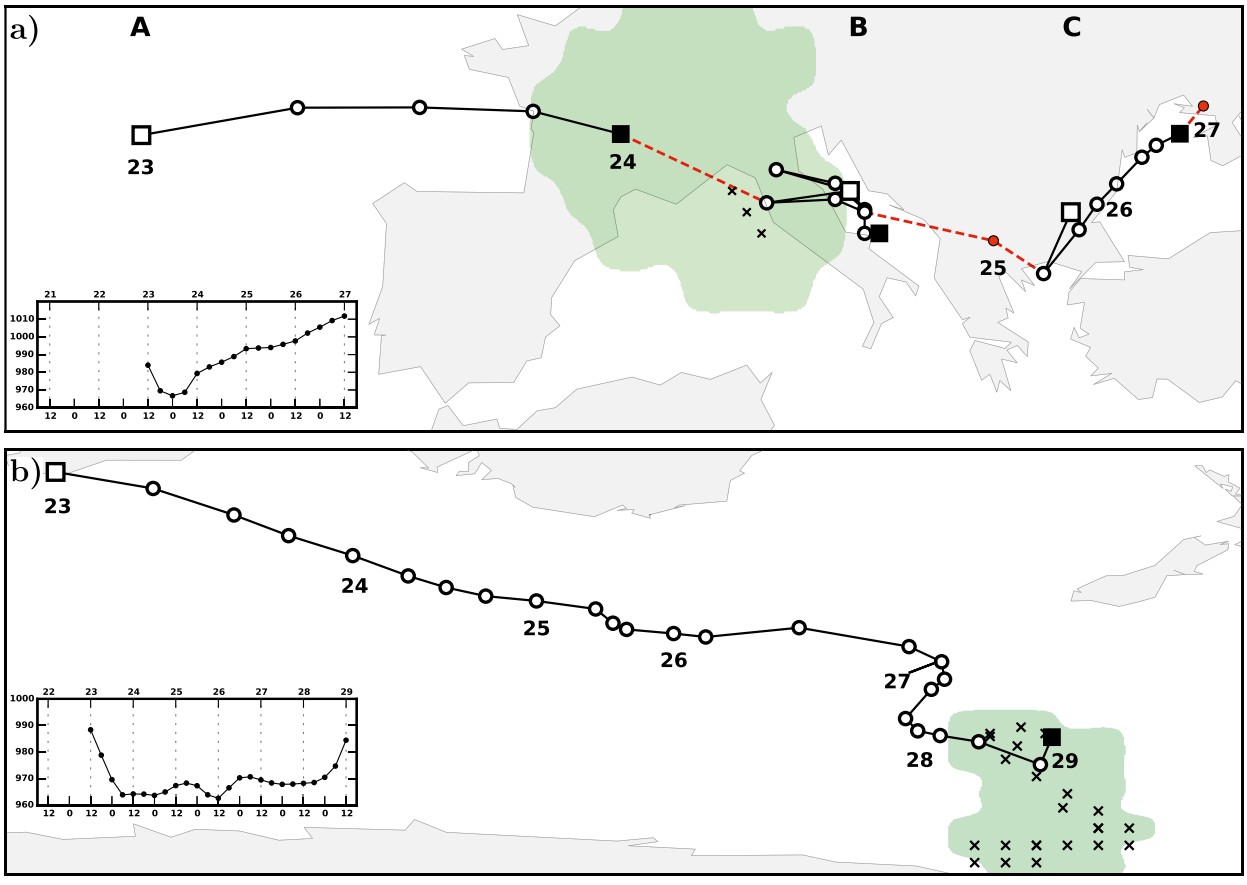


FIG. 2. (a) The MCMS three-track solution (A, B, and C) for the Klaus storm (22–27 Jan 2009). Each track trajectory follows a sequence of center markers (open square, a series of open circles, and ending in a filled square). The Xs mark select discarded centers at key points in the evolution of the storm. Green shading highlights the storm area of the final center in track A (day 24). A red dashed line, with red circle center markers, denotes where the alternative single-track solution departs from the three-track solution. An inset panel shows the time evolution of central SLP along the alternative track (the upper $x$ axis shows the day at 1200 UTC, which is also shown as a number under the appropriate track center, while the lower $x$ axis shows the UTC hour). (b) The unnamed storm (22–29 May 1994).

prevented the formation of track B. This change allowed MCMS to arrive at a single-track solution for the Klaus storm (red dotted line in Fig. 2a). This happened because former track A was then able to capture three key centers from former track B, plus a previously a discarded center over the Balkan Peninsula (red circle in Fig. 2a), which then acted as a bridge to incorporating most of former track C and even adding a final center at 0600 UTC 27 January near the Crimean Peninsula.

Clearly this kind of contingent and complex decision-making clouds the link between particular tracking outcomes and specific details of the tracking algorithm (Neu13). Indeed, even with the wealth of details provided by MCMS it remains unclear which basic parameters one would change, and by how much, to achieve a single-track solution for Klaus. Moreover, because changes to these parameters are universally applied, there is always the potential for large or unpredictable side effects.

For some applications the three-track fragmentation of Klaus is erroneous or at least detrimental, for example, works based on cyclone attributes such as duration or minimum lifetime SLP. For applications more concerned with centers than tracks such fragmentation is of less concern. For example, the single-track Klaus solution is mostly just a reorganization of the same pool of centers. Applications that treat centers as storm area are even less affected because the footprint of the enclosing SLP contours is larger than the differences in track/center specifics (green shaded area in Fig. 2a). In any event, we do not believe that excessive track fragmentation is a general problem for MCMS, but rather that the Klaus storm is a particularly problematic scenario for cyclone tracking (as was likely intended by Neu13).

The MCMS track for the second IMILAST storm, the unnamed cyclone of 22–29 May 1994, is shown in Fig. 2b. This storm was much less troublesome for MCMS.

Unauthenticated | Downloaded 03/15/22 04:05 PM UTC

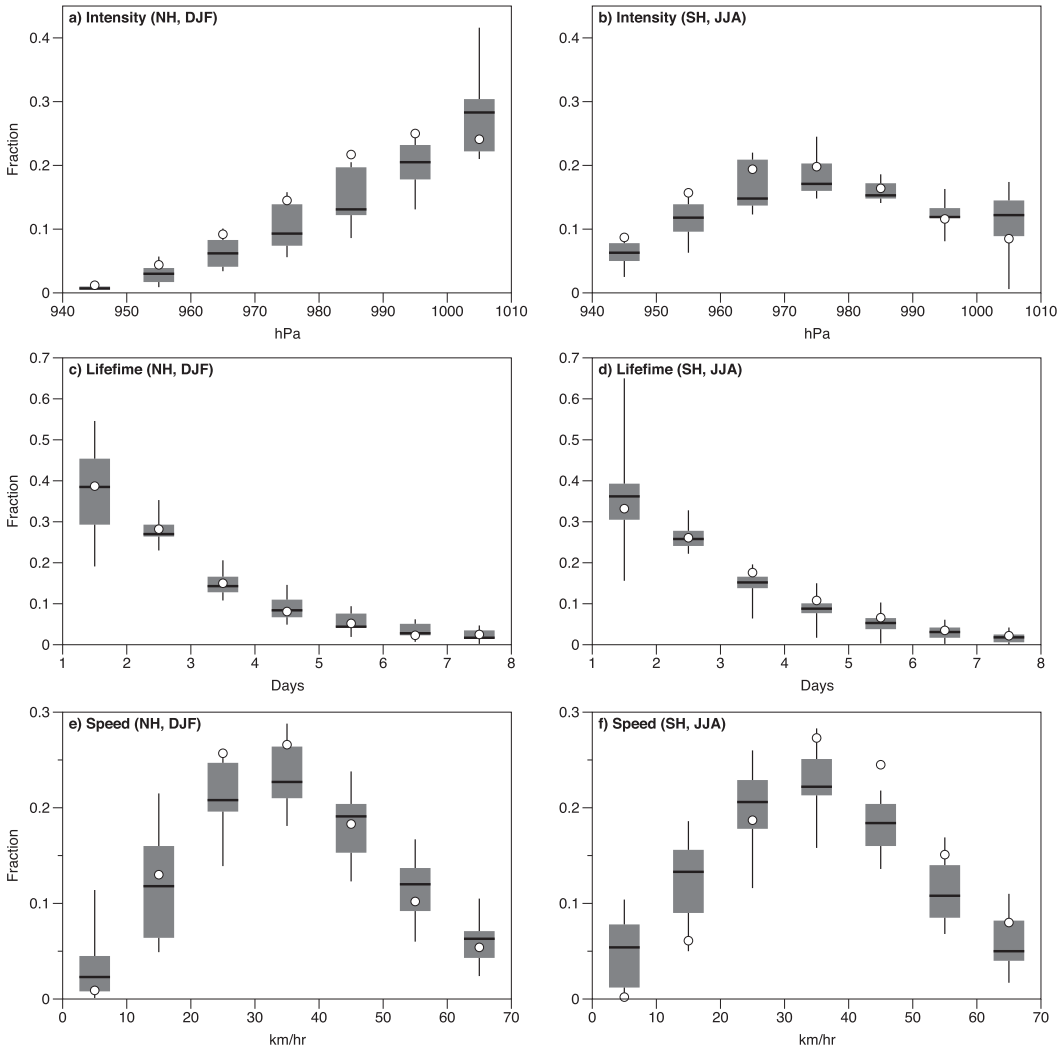


FIG. 3. Frequency distributions of select cyclone attributes: (a),(b) cyclone intensity (minimum lifetime SLP), (c),(d) cyclone lifetime, and (e),(f) track-average cyclone speed. The box-and-whisker plots represent the IMILAST population statistics (digitized from Fig. 3 in Neu13). Superimposed on these are the corresponding MCMS mean values (open circles).

Indeed, the default MCMS track closely corresponds to the longer tracks reported by IMILAST.

Taken together, these comparisons place MCMS within the inferred consensus tracks taken from the 15 IMILAST methods shown in Neu13 (their Figs. 4 and 5).

### 2) CYCLONE LIFE CYCLE

We will now explore the collective properties of the cyclones themselves. Our focus here is on the cyclone life cycle. As with Neu13, this analysis is limited to the cold-season cyclones from each hemisphere. In their study this is shown in a way that highlights the range of behavior among the 15 methods (their Fig. 3). We have reproduced this here in Fig. 3 along with comparable results from the restricted MCMS dataset noted earlier.

In general, Fig. 3 indicates that MCMS falls within the range of behavior exhibited by the IMILAST methods. There are nevertheless some differences of note. For example, MCMS has comparatively few weak intensity cyclones (Figs. 3a,b). However, this conclusion depends on the treatment of extreme centers whose intensities fall outside the histogram bounds of 940–1010 hPa. IMILAST ignores these extreme centers and reports the distribution seen in Figs. 3a and 3b. Because few MCMS centers reach pressures below 940 hPa, ignoring them has little effect on the histogram as a whole. This is not the case at the other end of the distribution, where MCMS reports a great number of centers just above the 1010-hPa cutoff. As a result, extending the bounds to just 1015 hPa lifts the MCMS mean value in the weakest

Unauthenticated | Downloaded 03/15/22 04:05 PM UTC

category to near the IMILAST mode and lowers the other means into the range reported by IMILAST.

The distribution of cyclone lifetime is comparatively well behaved, with MCMS closely following the IMILAST results at all intervals (Figs. 3c,d). This supports our earlier suggestion that track fragmentation is not a general problem for MCMS.

Last, we come to the distribution of track-mean cyclone speed (Figs. 3e,f). In this case, the degree of agreement with IMILAST depends on hemisphere. For example, MCMS reports relatively more NH cyclones at speeds between 10 and 40 km $h^{-1}$ and slightly fewer cyclones at higher speeds. The situation is somewhat reversed in the SH, where MCMS reports relatively fewer cyclones at speeds between 10 and 30 km $h^{-1}$ and more cyclones at higher speeds. MCMS finds fewer cyclones in the slowest category in both hemispheres. Unlike intensity, histogram boundary adjustments have little effect on the distribution of speed.

### 3) CLIMATOLOGY

Next we examine the climatological number and spatial distribution of MCMS and IMILAST cyclone tracks (restricted by topography and latitude). The IMILAST data for this come from Tables 2 and 3 in Neu13, and we use the method codes defined in their Table 1.

The general conclusion one can draw from this is that the MCMS track count falls close to the IMILAST method median for all seasons and hemispheres (Table 1).

A perhaps more informative view of these data comes when they are viewed as coordinate pairs (by method, hemisphere, and season; Fig. 4). Seen this way, it becomes clear that the various methods offer differing, and sometimes conflicting, characterizations of the cyclone activity present in the same data.

It is easily seen, for example, that some methods return many more tracks, or respond differently to season and hemisphere, than others. Neu13 noted this and suggested that a combination of detection differences, mostly related to shallow and open-wave systems, and rejection differences, mostly related to heat lows and other noncyclone low pressure areas, likely accounts for this dispersion. The NH warm season seems especially sensitive to these tracking differences (Neu13; Fig. 4). Indeed, disabling the MCMS filters targeting overly recurrent centers raises the MCMS track count during the NH warm season by about one-third without having much effect otherwise.

Although the absolute count differences shown in Fig. 4 can be large, it is also the case that most coordinate pairs fall near the 1:1 line. That is, both hemispheres have similar same-season track counts (e.g., cold season NH/SH). It is unclear if such symmetry is desirable, however. The possibility has not been ruled out, for example, that such symmetry simply reflects a biased sample from the relatively steady part of the cyclone distribution. If so, then some (or many) methods are too conservative. If not, then some aspects of the other methods are too permissive. Of course, the importance of this distinction depends on the questions being asked of the cyclone data. For now we point to the IMILAST project for future guidance in this area and note that even the methods with relatively large NH warm-season counts report a cold-season coordinate pair that is much closer to the 1:1 line.

TABLE 1. Total track count (hundreds of tracks) by season and hemisphere. The IMILAST method mean and median are shown beside the MCMS count (boldface type) with and without (the column with the asterisk) the IMILAST restrictions over high topography and low latitude (>1000 m, <30°).

| | | IMILAST | | MCMS | |
|---|---|---|---|---|---|
| | | Mean | Median | | * |
| NH | DJF | 124.6 ± 42.6 | — | **116.7** | **143.2** |
| | JJA | 150.2 ± 66.5 | 132.0 | **127.0** | **150.9** |
| SH | DJF | 104.4 ± 44.1 | 91.0 | **95.0** | **115.3** |
| | JJA | 110.4 ± 48.5 | 103.0 | **99.6** | **119.9** |

Figure 4 can also be viewed as a collection of method vectors that are directed from the cold to the warm season. From this we see that 11 of the 16 methods report more warm than cold-season tracks in the NH (i.e., the vector points up). Likewise, 10 of the 16 method vectors (including MCMS) report more cold- than warm-season tracks in the SH (i.e., vector points left).

The length and orientation of this vector reflects the amount and relative importance of hemispheric seasonality. That is, the longer the vector, the more the warm- and cold-season counts for that method differ. Likewise, the closer a vector aligns with either axis the more its seasonality represents just one hemisphere; here three methods fall within 30° of horizontal and are therefore SH dominant, while eight methods fall within 30° of vertical and are therefore NH dominant, and the remaining five methods (including MCMS) fall somewhere in between.

Together these results suggest that MCMS is among the least seasonal [14 of 16, closest to methods M14 (Kew et al. 2010) and M13 (Hanley and Caballero 2011)] and more hemispherically symmetric methods (all MCMS counts remain within 4% of each other). The MCMS track count falls close to the IMILAST method median for both hemispheres and globally. For the global count, MCMS falls closest to methods M10 (Simmonds et al. 2008) and M15 (Raible et al. 2008), while for the NH and SH counts, MCMS is closest to

Unauthenticated | Downloaded 03/15/22 04:05 PM UTC

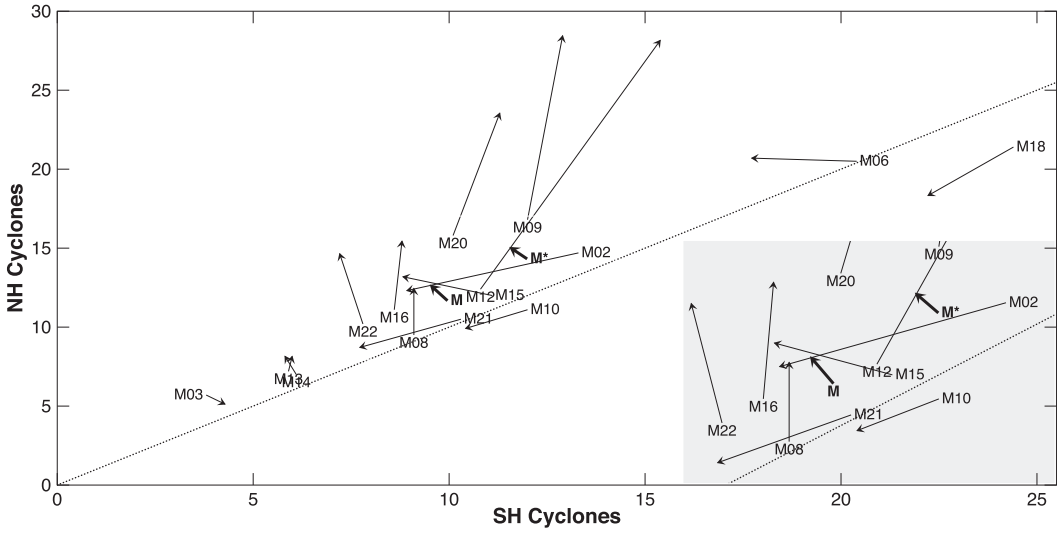


FIG. 4. Track count visualized by method and hemisphere using data from Neu13 (their Tables 2 and 3). Each method (labeled as in Neu13) is shown as coordinate pairs formed by the track count (×1000) from the Southern (SH, *x* axis) and Northern (NH, *y* axis) hemispheres. A vector points from the cold season toward the warm season. The corresponding MCMS result (M, thick arrow) falls within a cluster of results, whose detail is shown in an inset to the right (shaded). The MCMS result including all tracks is also shown (M*).

M15 and M22 (Akperov et al. 2007) and M15 and M08 (Trigo 2006), respectively. All but two methods report more NH than SH tracks (i.e., above the 1:1 line in Fig. 4). For MCMS, the NH count exceeds the SH count by about 25% (24 371 vs 19 462).

Lifting the IMILAST restrictions (i.e., using the normal MCMS data) increases the number of MCMS tracks by roughly 20% and does so a bit more in the NH (see Table 1). For the most part these extra tracks displace the MCMS vector without altering its other properties (see label M* in Fig. 4). This suggests that MCMS tracks that cross high topography are similar in character to other tracks.

Our final comparison with IMILAST concerns the spatial distribution of cyclone activity. A general issue here is that centers are sparsely distributed even in the storm tracks (i.e., points). The usual remedy for this is analogous to making a histogram in the sense that the centers are grouped over some larger area before being counted. In this case, the center counts are accumulated using an array of overlapping circular counting footprints (CDrad), which is customarily set to a radius of 5° latitude (the unit area). This count is the basis for an areal number density (or concentration) of cyclone centers, which can be normalized by the number of time steps to get a relative frequency (units: % occurrence per time step and per unit area). This field is called the center density (CD). For large samples CD represents the empirical likelihood of finding a nearby center. For example, a center density of 5% suggests that a cyclone center occurs near that point about once every 20 time steps (5 days).

The MCMS cold-season center density is shown in Fig. 5a. These patterns qualitatively agree with those of many IMILAST methods (Figs. 1 and 2 in Neu13). In terms of magnitude, the MCMS center densities fall about midrange of those reported by Neu13. This is consistent with our finding that MCMS center and track counts fall close to the IMILAST method median (i.e., Fig. 4 and Table 1). MCMS center densities are generally closest to methods M15 and M22. This is especially the case over the oceans.

## 3. Results

### *a. Center density*

In this section, we highlight a few general characteristics of MCMS-generated data. We begin by considering the two measures of climatological cyclone activity reported by the MCMS software. The first of these is the aforementioned CD, which is a widely reported measure of areal center concentration (i.e., SLP minima, Fig. 5a). The MCMS software offers another related measure, storm-area density (AD), which represents the areal concentration of the enclosed area found around cyclone centers (i.e., closed SLP contours, Fig. 5b).

Storm-area density is accrued much like center density except that each center's contribution reflects its SArea. Using Fig. 1b as a reference, this amounts to incrementing the concentration everywhere a color-shaded area

Unauthenticated | Downloaded 03/15/22 04:05 PM UTC

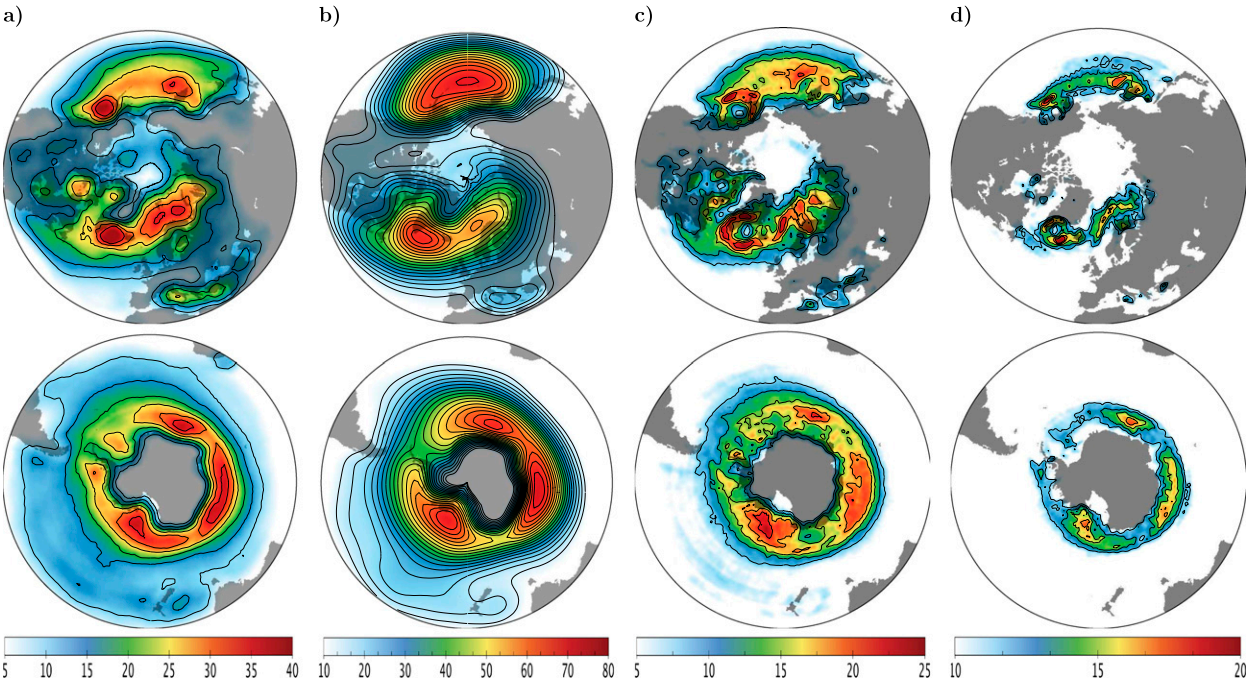


FIG. 5. Measures of wintertime cyclone activity (ERAi): (top) NH in DJF and (bottom) SH in JJA. (a) CD computed with a default CDrad of 5° lat [center occurrence (%) per unit area and time]. (b) AD [SArea occurrence (%) per unit area and time]. The CD difference (larger − smaller) using a CDrad, which roughly (c) doubles (~7° lat) and (d) halves (~3.5° lat) the default radius.

overlaps with a counting footprint (CDrad). This fractional overlap is used to weight each footprint count (e.g., +0.1 for 10% overlap rather than +1). For large samples, AD approximates the empirical likelihood of finding some SArea nearby [SArea occurrence (%) per unit area per unit time]. In other words, AD represents the likelihood that a given location is influenced by a cyclone. An AD value of 5% suggests that some SArea occurs near that point about once every 20 time steps (5 days).

The degree to which these two density measures resemble one another largely depends on how much and how often SArea conforms to the geometry of CDrad. There are three geometric attributes to consider here: size, shape, and symmetry. Of these, size has the most leverage over CD and AD.

To test for CDrad dependencies we doubled and halved the footprint area and recalculated CD (e.g., CDrad of ~7° and ~3.5°; Figs. 5c,d). As expected, reducing CDrad leads to a more fragmented distribution, while enlarging it smooths and raises the overall magnitude (i.e., analogous to changing a histogram's bin width). The CD peaks of the North Pacific Ocean and, to a lesser extent, of the North Atlantic Ocean are especially sensitive to footprint size because of the placement and strength of gradients in the land–sea distribution of centers there. For example, switching to the largest CDrad makes the North Pacific peaks broader, less distinct, and closer together, whereas switching to the smallest CDrad has the opposite effect (Figs. 5a,c,d).

### b. *Storm-area density*

We now turn to AD. In contrast to CD, AD is comparatively insensitive to the choice of CDrad. Two details concerning the calculation of AD account for this robustness: 1) AD tallies areas rather than points (i.e., centers), and 2) the AD tally is weighted by the fractional overlap with each footprint. The first factor ensures that a certain amount of areal smoothing occurs even when CDrad is small. The second factor limits the potential of oversmoothing even when CDrad is large.

Storm-area density is also insensitive to the contour interval that is used to delineate SArea (over the range of 0.5–2.0 hPa). Shallow centers (depressions) are the most sensitive to the contour interval because it affects whether they are classified as being empty or not (no closed contours).

There are, however, indications that closed SLP contours are somehow constrained in extent over land (e.g., by the topographic distortion of the pressure field or limitations with the MCMS software). For example, the land/sea distributions of SArea in the NH exhibit systematic differences such that land-based centers are smaller and more apt to be empty, and MCC are both

Unauthenticated | Downloaded 03/15/22 04:05 PM UTC

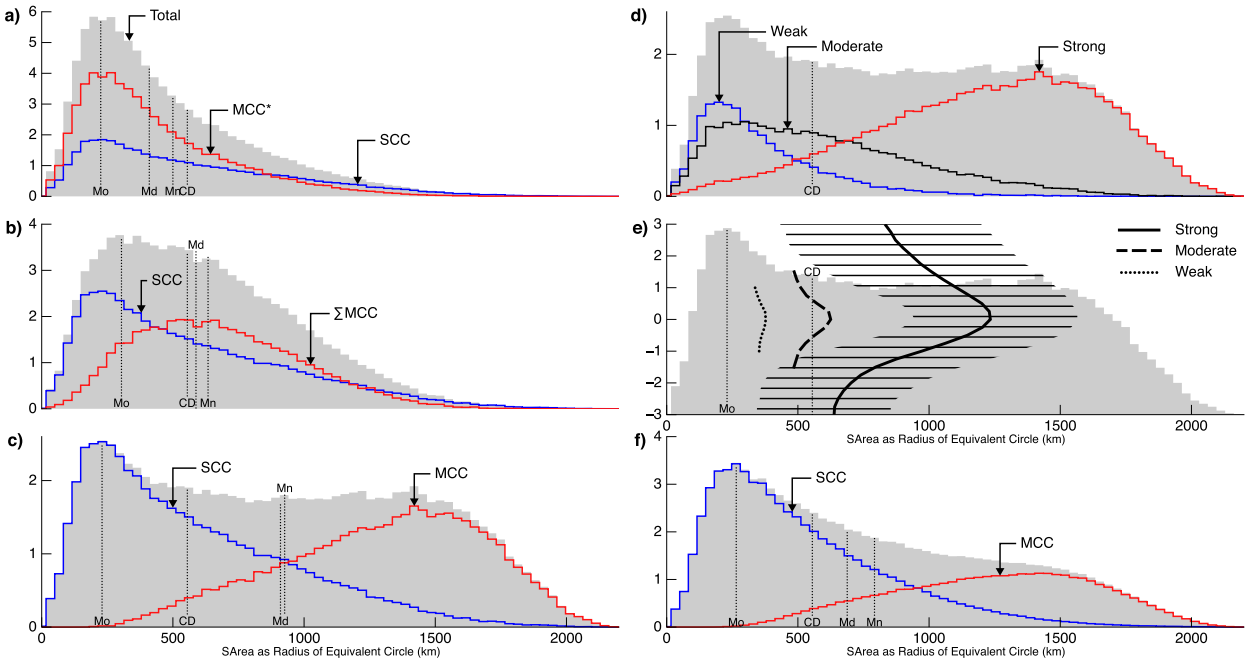


FIG. 6. Frequency histograms of SArea (global, annual). SCC and MCC partitions are shown on most panels (scaled as percentage of total). The left column shows three ways of accounting for MCC SArea (SCC unchanged in absolute terms): (a) Treat embedded centers separately (MCC*). (b) Sum embedded centers by system (ΣMCC). (c) Include the area between embedded centers (MCC). (d) Restatement of (c), but partitioned by peak track intensity (weak, moderate, or strong). (e) Life cycle variations of SArea. The *x* axis is the same as before (total shown for comparison). A new *y* axis marks time (days) relative to when peak track SArea was reached by each cyclone. Three vertical curves depict the time evolution of mean SArea (time moving upward) by intensity. The displayed time span for each intensity class is limited to the approximate time when the center count falls below 25% of the peak count. The interquartile range for just the strong intensity class is shown (horizontal lines). (f) Restatement of (c) using all centers. All panels [except (f)] show the distribution of peak track SArea (total). Many panels have vertical lines marking the mean (Mn), median (Md), mode (Mo), and, for reference, CD.

rarer and smaller as well. On the other hand, cyclone size covaries to some degree with other cyclone attributes such as life cycle and intensity (e.g., Grotjahn et al. 1999; Simmonds 2000; Rudeva and Gulev 2007; Rudeva 2008; Schneidereit et al. 2010). Thus, it is also possible that these land/sea differences are simply manifestations of similar contrasts among the many influences shaping cyclone activity and size.

This leaves the treatment of MCC cyclone systems as the last important procedural consideration related to the calculation of AD. There are two basic options to consider here. The first option fuses each MCC into a single storm area before counting (the primary center). MCMS uses this tactic by default (e.g., for Fig. 5b). The second option simply counts storm area as if every center were an SCC (i.e., ignore SArea_Shared, just the red areas in Fig. 1b). While the spatial pattern of AD is largely unaffected by this change, its magnitude is reduced by more than half, which brings it closer to CD. This in-place magnitude reduction suggests that MCC storm area is mostly SArea_Shared.

One can see this more clearly by repeating the above exercise using histograms of SArea (Fig. 6). As before, we initially treat all centers as SCC (dismantled MCC denoted as MCC*). A key conclusion here is that MCC differ from SCC even when viewed as single-center storm areas (Fig. 6a). For example, relatively more MCC* fall near the pronounced modal peak (~300 km) and relatively fewer occur at sizes larger than about 800 km. These findings are consistent with the idea that MCC systems typically consist of a larger primary center (larger, not necessarily large) and one or two relatively smaller secondary centers. In other words, the MCC* distribution represents two center populations.

Accumulating MCC* on a system-by-system basis (here ΣMCC) simply redistributes the same area to larger sizes (SCC unchanged in absolute terms, Fig. 6b and Table 2). The addition of SArea_Shared in contrast, shifts the entire MCC distribution toward larger sizes and effectively flattens the overall SArea distribution except near its extremities (Fig. 6c, Table 2). This

Unauthenticated | Downloaded 03/15/22 04:05 PM UTC

TABLE 2. Summary statistics related to the track-maximum storm area in Figs. 6a–c. Standard central tendency measures are shown (radius of equivalent circle; km), as are the percent of all centers and storm area accounted for by MCC.

| | SCC | MCC* | ΣMCC | MCC |
|---|---|---|---|---|
| Mean | 586 | 446 | 689 | 1315 |
| Median | 499 | 377 | 666 | 1354 |
| Mode | 243 | 273 | 553 | 1441 |
| % centers | — | 61.3 | 46.5 | 46.5 |
| % area | — | 47.2 | 47.2 | 77.0 |

reconfirms the idea that MCC storm area is mostly SArea_Shared.

We will now use Fig. 6 to explore how cyclone development and life cycle affect storm area. This requires some measure of cyclone intensity. For this we used the ranked zonal SLP anomaly of each MCC primary and SCC center (i.e., percentiles). In this way, <10% of all the centers from a given month and hemisphere will have a larger (i.e., stronger) anomaly than a center from the 90th percentile. The 33rd and 66th percentiles were then used to form three broad intensity categories (weak, moderate, and strong). Overall, this measure of cyclone intensity is less sensitive to hemisphere and season than one based directly on SLP.

Sorting SArea by intensity shows that larger cyclones also tend to reach higher intensities (Fig. 6d). Small, strong storms are a notable exception to this pattern. On closer examination we find that these SCC are mostly tropical storms (e.g., hurricanes).

The prominence of large MCC dwindles once the entire cyclone life history is considered (rather than just at peak SArea; cf. Figs. 6c and 6f). Painted in broad brushstrokes, this number disparity (many small and fewer large centers) is related to the variation of cyclone intensity over the cyclone life cycle (i.e., size linked to development).

To see this, we rearranged SArea around the time at which each cyclone track reached maximum intensity (Fig. 6e). This shows that cyclones largely follow a characteristic pattern of growth and decay over their life cycle (vertical curves in Fig. 6e). Simmonds and Keay (2000) and Rudeva and Gulev (2007) report a comparable progression of cyclone size over the cyclone life cycle.

There is considerable spread, and some overlap, when these patterns are sorted by peak cyclone intensity. This intensity sensitivity is especially evident during the early and late stages of cyclone development. Because of this, even cyclones that eventually reach high intensity and large size can contribute to the population of small centers (horizontal lines in Fig. 6e). In contrast, many lower intensity cyclones remain small over their entire life cycle and thus only add to the abundance of small centers.

Unlike the small-size end of the SArea distribution, which is remarkably invariant, the large-size tail varies with season and hemisphere. This size variation is mostly tied to MCC and is the likely cause for the hemispheric and seasonal contrast between CD and AD found near the semipermanent lows.

## 4. Discussion

The NASA Modeling, Analysis, and Prediction (MAP) Climatology of Mid-Latitude Storm Area (MCMS) is a tool for finding, tracking, and delineating midlatitude cyclones in gridded data. This results in a detailed life history for each captured cyclone including estimates of its position, trajectory, and geometry.

A few distinctive features of the MCMS method were highlighted here. For example, the MCMS software adjusts key parameters to the dataset being analyzed and generates extensive diagnostics for every operation. The MCMS software also addresses problematic situations related to the use of SLP extrema as a way of finding candidate cyclone centers. Foremost among these challenges are excessively recurrent low pressure areas (e.g., heat lows) and open-wave cyclone patterns. MCMS track finding introduces the ability to reconsider candidate cyclone centers previously rejected by the many filters used by the MCMS algorithm (e.g., rejected heat lows). Likewise, the pool of rejected tracks is tested for centers that can be used to extend or improve the final set of retained tracks. Finally, the MCMS software locates the outermost closed SLP contour around each retained cyclone center as a way to delineate its extent (size and shape) and to decide if it belongs to a multicenter system.

Collectively, MCMS data were shown to be broadly consistent with the 15 cyclone-finding methods surveyed by IMILAST (Neu13). This similarity was explored at several levels of detail. For example, we examined individual cyclones using the two case studies provided by IMILAST (Fig. 2). In each case, the wealth of diagnostic information retained by the MCMS data allowed us to untangle the complex interplay between the MCMS algorithm and the circumstances presented by each scenario. Details related to the collective properties of MCMS and IMILAST cyclones were also explored and found to be comparable (e.g., Figs. 3 and 5a).

The stability of MCMS center/track counts across season and hemisphere, especially relative to their absolute numbers, is perhaps the most distinctive quality of

Unauthenticated | Downloaded 03/15/22 04:05 PM UTC

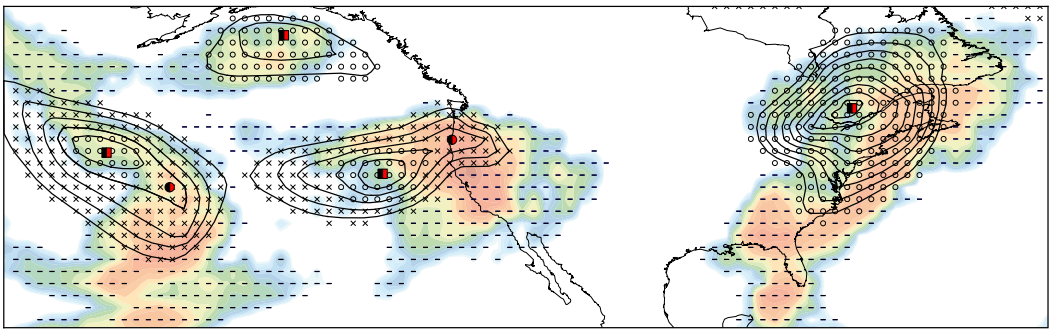

FIG. 7. Cyclone-related precipitation from the GPCP identified with ERAi-based MCMS data. The daily precipitation rate from GPCP is shown on a blue-to-red log scale for values of 1–100 mm day$^{-1}$ (25 Jan 1997). Superimposed on this are the corresponding SCC and MCC-primary centers (black and red boxes) and MCC-secondary centers (black and red circles). The associated MCMS storm areas for these centers are roughly indicated by contours, with areas linked to individual centers shown as open circles and those shared among MCC with Xs. An additional capture of cyclone-related precipitation outside these storm areas is shown as dashes.

MCMS in this regard (Fig. 4 and Table 1). A sharp increase in track count during the NH warm season prevents many IMILAST methodologies from sharing this quality. For this reason, we suspect that the special efforts the MCMS software takes to confront problematic situations, such as those over high or steep topography, account for the robustness of the MCMS result. Indeed, MCMS retains this status even when the centers/tracks it finds over high topography are included (M and M* in Fig. 4).

We also compared two measures of climatological cyclone activity: the widely used center density (CD) and storm-area density (AD). Our overall conclusion is that these measures are complementary, with one being insensitive to variations in storm area (CD) while the other incorporates it (AD).

It is important to realize that the patterns of CD and AD can differ. Indeed, they are only the same when storm area often matches the CD collection footprint, which it generally does not, as Fig. 6f shows. Conversely, AD could deviate greatly from CD if storm area were arbitrary. However, Fig. 5 argues against this possibility.

It seems likely then that the relationship between CD and AD is conditional on other factors. A prime candidate here is the process of cyclone development. For example, cyclone size and intensity roughly covary over the cyclone life cycle (Figs. 6d,e; Simmonds and Keay 2000; Rudeva and Gulev 2007). This progression also exhibits a loose spatial organization with well-known regions for preferred genesis, intensification, and lysis. In this way, smaller, faster-moving single-center cyclones tend to occur at lower latitudes (low CD and AD), while larger, slower-moving multicenter cyclones are more common at higher latitudes (high CD and AD).

Figure 6 suggests that most cyclone centers come from what is arguably the least certain part of the cyclone distribution, not only for cyclone finding, but also for modeling and retention in gridded SLP data: small, shallow depressions, many of which occur during the earliest and latest stages of cyclone development. It is thus prudent to consider the problem of cyclone representation whenever interpreting center density differences among datasets or within a single dataset over time (i.e., shifts in the local mix of center types over time or between datasets).

We envision MCMS as a community tool for the general investigation of extratropical cyclones and their area of influence (storm area). A few of the many potential uses have been demonstrated here (e.g., Figs. 5 and 6). When discussing these figures the point was raised that accounting for the areal extent of individual cyclones is both important and useful.

Admittedly, the correctness of this statement depends on its application. For example, frontal precipitation and cloud are unlikely to be wholly confined to the storm-area boundaries ascribed by the MCMS software. However, even in these cases MCMS data can be useful. Figure 7 demonstrates a simple method for capturing daily precipitation observations provided by the Global Precipitation Climatology Project using MCMS data (GPCP, 1DD v1.2; Huffman et al. 2001). To start, we mapped concurrent MCMS storm areas and GPCP data onto a common data grid (here 25 January 1997). Because the GPCP data are daily and the ERAi MCMS data are 6-hourly, we opted to use the subdaily storm areas that enclosed the most precipitation (1800 UTC). Figure 7 depicts these storm areas as open circles (areas unique to one center) and Xs (shared areas). We then initiated a nearest-neighbor search for precipitating

Unauthenticated | Downloaded 03/15/22 04:05 PM UTC

grids along the perimeter of each storm area. Newly found precipitating grids then served as seeds for a new search and so on. This process continued until no new precipitating grids were added or one of three stop conditions was reached. The first stop condition prevented searches from extending into the storm areas of cyclones other than the one at the root of the search tree. The second stop condition limited searches to a 3000-km radius of the root cyclone. For root cyclones that were members of a multicenter system, this condition was interpreted to mean within a 3000-km radius of any member center. The final stop condition limited searches to the extratropics (>20° latitude). Figure 7 depicts these extended search results as dashes.

The analysis depicted in Fig. 7 clearly improves the GPCP capture over that provided by the MCMS data alone. It is also easy to see how the adaptive nature of the extended MCMS capture might be superior to those used in more traditional methods such as weather states and cyclone-centric composites (e.g., Tselioudis et al. 2000; Bauer and del Genio 2006; Field and Wood 2007). That is, the fixed spatial collection domain (i.e., box) usually used by these methods is poorly suited to the variable precipitation patterns shown in Fig. 7.

MCMS data from several reanalysis efforts will be made publicly available. MCMS data come in the form of specially formatted plain text files. The formatting of these files is well documented and easily expressed in most programming languages. In addition, MCMS provides tools for manipulating and analyzing the information it produces. For example, these tools can create a gridded netCDF file from MCMS center and storm-area data. For those interested in creating new MCMS datasets (e.g., center finding, tracking, and delineation), we offer the full suite of MCMS source code (written in Python). Users can freely modify, improve, and extend the MCMS software and are encouraged to make these changes available to the wider community. Information about the MCMS data and software and how to obtain and use them is located online (http://gcss-dime.giss.nasa.gov/mcms/).

*Acknowledgments.* Work by all authors was supported in part by the NASA Modeling and Analysis Program (managed by Dr. David Considine) under Grants 08MAP0004 and NNXD7AN04G and by NSF 1240643 from PO-06-5740 (Dr. Eric DeWeaver). The ERA-Interim reanalysis pressure fields were provided by the European Centre for Medium-Range Weather Forecasts (ECMWF) and obtained from their data server (http://www.ecmwf.int/en/research/climate-reanalysis/era-interim). We also express our gratitude to the numerous reviewers and editors for their generosity of time and effort. Their many contributions and corrections made this a much better article and reminded us that good science is often a community effort.

## REFERENCES

Akperov, M., M. Bardin, E. Volodin, G. Golitsyn, and I. Mokhov, 2007: Probability distributions for cyclones and anticyclones from the NCEP/NCAR reanalysis data and the INM RAS climate model. *Izv. Atmos. Ocean. Phys.*, **43**, 705–712, doi:10.1134/S0001433807060047.

Bauer, M., and A. del Genio, 2006: Composite analysis of winter cyclones in a GCM: Influence on climatological humidity. *J. Climate*, **19**, 1652–1672, doi:10.1175/JCLI3690.1.

Dee, D., and Coauthors, 2011: The ERA-Interim reanalysis: Configuration and performance of the data assimilation system. *Quart. J. Roy. Meteor. Soc.*, **137**, 553–597, doi:10.1002/qj.828.

Field, P., and R. Wood, 2007: Precipitation and cloud structure in midlatitude cyclones. *J. Climate*, **20**, 233–254, doi:10.1175/JCLI3998.1.

Grotjahn, R., D. Hodyss, and C. Castello, 1999: Do frontal cyclones change size? Observed widths of North Pacific lows. *Mon. Wea. Rev.*, **127**, 1089–1095, doi:10.1175/1520-0493(1999)127<1089:DFCCSO>2.0.CO;2.

Hanley, J., and R. Caballero, 2011: Objective identification and tracking of multicentre cyclones in the ERA-Interim reanalysis dataset. *Quart. J. Roy. Meteor. Soc.*, **138**, 612–625, doi:10.1002/qj.948.

Hawcroft, M. K., L. C. Shaffrey, K. I. Hodges, and H. F. Dacre, 2012: How much Northern Hemisphere precipitation is associated with extratropical cyclones? *Geophys. Res. Lett.*, **39**, L24809, doi:10.1029/2012GL053866.

Hewson, T., 2009: Diminutive frontal waves—A link between fronts and cyclones. *J. Atmos. Sci.*, **66**, 116–132, doi:10.1175/2008JAS2719.1.

Hodges, K., 1999: Adaptive constraints for feature tracking. *Mon. Wea. Rev.*, **127**, 1362–1373, doi:10.1175/1520-0493(1999)127<1362:ACFFT>2.0.CO;2.

Hoskins, B., and K. Hodges, 2002: New perspectives on the Northern Hemisphere winter storm tracks. *J. Atmos. Sci.*, **59**, 1041–1061, doi:10.1175/1520-0469(2002)059<1041:NPOTNH>2.0.CO;2.

Huffman, G. J., R. F. Adler, M. M. Morrissey, D. T. Bolvin, S. Curtis, R. Joyce, B. McGavock, and J. Susskind, 2001: Global precipitation at one-degree daily resolution from multisatellite observations. *J. Hydrometeor.*, **2**, 36–50, doi:10.1175/1525-7541(2001)002<0036:GPAODD>2.0.CO;2.

Inatsu, M., 2009: The neighbor enclosed area tracking algorithm for extratropical wintertime cyclones. *Atmos. Sci. Lett.*, **10**, 267–272, doi:10.1002/asl.238.

Kew, S. F., M. Sprenger, and H. C. Davies, 2010: Potential vorticity anomalies of the lowermost stratosphere: A 10-yr winter climatology. *Mon. Wea. Rev.*, **138**, 1234–1249, doi:10.1175/2009MWR3193.1.

Kimball, S. K., and M. S. Mulekar, 2004: A 15-year climatology of North Atlantic tropical cyclones. Part I: Size parameters. *J. Climate*, **17**, 3555–3575, doi:10.1175/1520-0442(2004)017<3555:AYCONA>2.0.CO;2.

Liberato, M. L. R., J. G. Pinto, I. F. Trigo, and R. M. Trigo, 2011: Klaus—An exceptional winter storm over northern Iberia and southern France. *Weather*, **66**, 330–334, doi:10.1002/wea.755.

Unauthenticated | Downloaded 03/15/22 04:05 PM UTC

Merrill, R. T., 1984: A comparison of large and small tropical cyclones. *Mon. Wea. Rev.*, **112**, 1408–1418, doi:10.1175/1520-0493(1984)112<1408:ACOLAS>2.0.CO;2.

Murray, R., and I. Simmonds, 1991: A numerical scheme for tracking cyclone centres from digital data. Part 1: Development and operation of the scheme. *Aust. Meteor. Mag.*, **39** (3), 155–166.

Neu, U., and Coauthors, 2013: IMILAST: A community effort to intercompare extratropical cyclone detection and tracking algorithms. *Bull. Amer. Meteor. Soc.*, **94**, 529–547, doi:10.1175/BAMS-D-11-00154.1.

Pfahl, S., and H. Wernli, 2012: Quantifying the relevance of cyclones for precipitation extremes. *J. Climate*, **25**, 6770–6780, doi:10.1175/JCLI-D-11-00705.1.

Raible, C. C., P. M. Della-Marta, C. Schwierz, H. Wernli, and R. Blender, 2008: Northern Hemisphere extratropical cyclones: A comparison of detection and tracking methods and different reanalyses. *Mon. Wea. Rev.*, **136**, 880–897, doi:10.1175/2007MWR2143.1.

Romanski, J., A. Romanou, M. Bauer, and G. Tselioudis, 2012: Atmospheric forcing of the Eastern Mediterranean Transient by midlatitude cyclones. *Geophys. Res. Lett.*, **39**, L03703, doi:10.1029/2011GL050298.

Rudeva, I., 2008: On the relation of the number of extratropical cyclones to their sizes. *Izv. Atmos. Ocean Phys.*, **44**, 273–278, doi:10.1134/S000143380803002X.

——, and S. K. Gulev, 2007: Climatology of cyclone size characteristics and their changes during the cyclone life cycle. *Mon. Wea. Rev.*, **135**, 2568–2587, doi:10.1175/MWR3420.1.

Sanders, F., and J. R. Gyakum, 1980: Synoptic-dynamic climatology of the ''bomb.'' *Mon. Wea. Rev.*, **108**, 1589–1605, doi:10.1175/1520-0493(1980)108<1589:SDCOT>2.0.CO;2.

Schneidereit, A., R. Blender, and K. Fraedrich, 2010: A radius-depth model for midlatitude cyclones in reanalysis data and simulations. *Quart. J. Roy. Meteor. Soc.*, **136**, 50–60, doi:10.1002/qj.523.

Simmonds, I., 2000: Size changes over the life of sea level cyclones in the NCEP reanalysis. *Mon. Wea. Rev.*, **128**, 4118–4125, doi:10.1175/1520-0493(2000)129<4118:SCOTLO>2.0.CO;2.

——, and K. Keay, 2000: Mean Southern Hemisphere extratropical cyclone behavior in the 40-year NCEP–NCAR Reanalysis. *J. Climate*, **13**, 873–885, doi:10.1175/1520-0442(2000)013<0873:MSHECB>2.0.CO;2.

——, C. Burke, and K. Keay, 2008: Arctic climate change as manifest in cyclone behavior. *J. Climate*, **21**, 5777–5796, doi:10.1175/2008JCLI2366.1.

Sinclair, M., 1994: An objective cyclone climatology for the Southern Hemisphere. *Mon. Wea. Rev.*, **122**, 2239–2256, doi:10.1175/1520-0493(1994)122<2239:AOCCFT>2.0.CO;2.

Trigo, I. F., 2006: Climatology and interannual variability of storm-tracks in the Euro-Atlantic sector: A comparison between ERA-40 and NCEP/NCAR reanalyses. *Climate Dyn.*, **26**, 127–143, doi:10.1007/s00382-005-0065-9.

Tselioudis, G., Y. Zhang, and W. B. Rossow, 2000: Cloud and radiation variations associated with northern midlatitude low and high sea level pressure regimes. *J. Climate*, **13**, 312–327, doi:10.1175/1520-0442(2000)013<0312:CARVAW>2.0.CO;2.

Wang, X., V. Swail, and F. Zwiers, 2006: Climatology and changes of extratropical cyclone activity: Comparison of ERA-40 with NCEP–NCAR reanalysis for 1958–2001. *J. Climate*, **19**, 3145–3166, doi:10.1175/JCLI3781.1.

Wernli, H., and C. Schwierz, 2006: Surface cyclones in the ERA-40 dataset (1958–2001). Part I: Novel identification method and global climatology. *J. Atmos. Sci.*, **63**, 2486–2507, doi:10.1175/JAS3766.1.

Unauthenticated | Downloaded 03/15/22 04:05 PM UTC